
Image Captioners Are Scalable Vision Learners Too

Michael Tschannen^{○,†} Manoj Kumar[○] Andreas Steiner[○]
 Xiaohua Zhai Neil Houlsby Lucas Beyer[○]
 Google DeepMind

Abstract

Contrastive pretraining on image-text pairs from the web is one of the most popular large-scale pretraining strategies for vision backbones, especially in the context of large multimodal models. At the same time, image captioning on this type of data is commonly considered an inferior pretraining strategy. In this paper, we perform a fair comparison of these two pretraining strategies, carefully matching training data, compute, and model capacity. Using a standard encoder-decoder transformer, we find that captioning alone is surprisingly effective: on classification tasks, captioning produces vision encoders competitive with contrastively pretrained encoders, while surpassing them on vision & language tasks. We further analyze the effect of the model architecture and scale, as well as the pretraining data on the representation quality, and find that captioning exhibits the same or better scaling behavior along these axes. Overall our results show that plain image captioning is a more powerful pretraining strategy than was previously believed.

1 Introduction

Contrastive language image pretraining (CLIP) [48] has recently become a very popular pretraining strategy, enabling scalable vision-language pretraining on billions of image-text pairs collected from the web. CLIP not only enables zero-shot transfer to arbitrary image classification and retrieval tasks, but also produces high-quality vision backbones rivaling the best label-supervised ones [14]. The corresponding checkpoints [48, 9, 56] are among the most powerful publicly available vision backbones, enjoying wide adoption in the context of multi-modal vision-language models, where often a pretrained vision backbone is combined with a pretrained language model [1, 6, 60, 22, 17, 5].

Before contrastive image-text pretraining was popularized by CLIP [48] and ALIGN [25], a number of works explored generative image captioning [13, 52] and n-gram prediction [26, 36] approaches for representation learning at small scale. However, [48] showed that the zero-shot classification performance of contrastive pretraining scales much better than captioning as a function of the number of training examples seen (see [48, Fig. 2]). Since then, follow-up works of [48] which focus on pretraining from scratch do usually not rely on captioning alone, but augment it with a contrastive loss [64, 33, 39]. Those follow-up works based on generative captioning alone typically rely on cross-modal encoders with early fusion of image and text, targeting visual question answering (VQA) and/or captioning tasks with the full encoder-decoder system [61, 21, 10], and do not study the properties of the vision backbone alone.

We revisit image captioning as a pretraining task for learning general vision encoders from web image-text pairs. We compare CLIP-style models with image captioning ones consisting of a Vision Transformer (ViT) [15] encoder and a standard Transformer decoder, henceforth simply referred to as Captioner (Cap). In our experiments, we carefully match pretraining compute and model capacity, and train both models for the same number of examples.

[○]Significant technical contributions. [†]MT led the project.

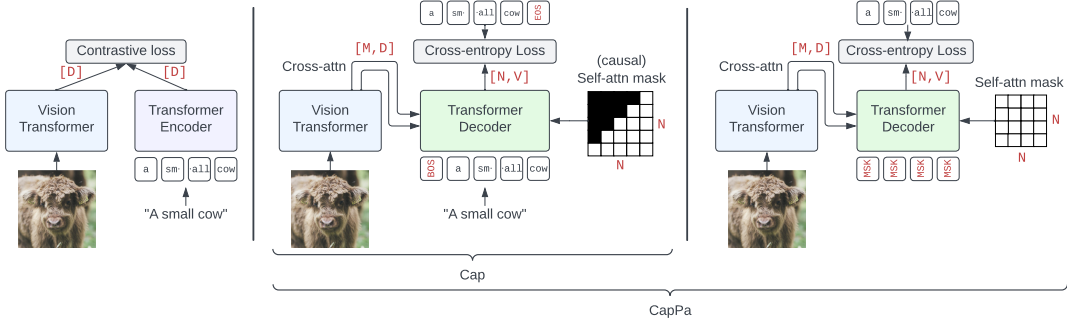


Figure 1: Contrastive models (**left**) use two separate Transformer encoders to extract vector representations from image-text pairs, which are then matched across a potentially large batch [48]. Cap (**middle**) uses a Transformer encoder-decoder architecture [58] and predicts text tokens autoregressively. During training, all tokens are predicted in parallel by shifting the expected output by one token and applying a causal self-attention mask (teacher forcing). In *parallel* decoding (**right**) the Transformer decoder has to predict all tokens at once, conditioned only on the image. CapPa trains a single model switching between autoregressive and parallel decoding.

D : model width, M : number of image tokens, N : number of text tokens, V : vocabulary size.

While our results confirm the findings of [48] that Cap models generally lag contrastive ones in zero-shot classification accuracy, the gap becomes smaller with increasing scale. More importantly, the Cap vision backbone matches or outperforms comparable CLIP models in few-shot classification and obtains competitive performance when transferring to classification tasks with large labeled data sets. When combining the vision encoder with a randomly initialized transformer decoder, the Cap pretrained encoder outperforms the CLIP one on captioning, OCR, and VQA tasks. This indicates that a Cap vision backbone might be better suited for multimodal downstream tasks. These benefits can be even more pronounced when combining the vision encoder with a pretrained, partially frozen language decoder similar to [1, 6, 60, 22, 17, 5].

We further propose the CapPa pretraining procedure: the decoder training alternates between standard autoregressive prediction (Cap) and *parallel* prediction (Pa), where the entire caption is predicted in a single decoder forward pass. This only changes the decoder text input (all input tokens are set to [MASK] tokens) and self-attention mask (no mask instead of a causal mask) while requiring no change in the loss or architecture. This mixed training, termed CapPa, significantly improves classification accuracy of the vision backbone.

We ablate how various training and architecture design choices impact performance, and discover promising scaling properties of captioners. Finally, we show that Cap achieves state-of-the-art performance in zero-shot classification tasks which require careful handling of word order and attributes, rather than treating the query as a bag-of-words, as measured by the ARO benchmark [65].

Overall, our results show that pretraining a simple encoder-decoder architecture via image captioning alone can produce vision encoders competitive with CLIP and presents an interesting alternative to contrastive pretraining—in particular for multimodal vision-language models built from pretrained vision and language modeling components.

2 Related work

Large scale contrastive vision-language pretraining was popularized by CLIP [48] and ALIGN [25]. Several works investigated scaling beyond these works along several relevant axes [47, 67] or using pretrained vision and language backbones with contrastive training [68].

Recent works investigating plain image captioning for pretraining are [13, 52]; [26, 36] study n-gram prediction from images, which can be considered a precursor to captioning. However, image captioning as a pretraining task to learn general vision representations did not attract as much attention as contrastive training, possibly because of inferior and less efficient zero-shot transfer capabilities. Related to captioning, SimVLM [61] uses prefix language modeling to pretrain a multimodal encoder-

decoder model with early vision-language fusion and hybrid convolutional/transformer vision encoder, targeting transfer to VQA and captioning. Further, encoder-decoder models for document, website, and UI understanding are often pretrained to generate captions from rendered websites/documents which trains the model to extract features from those data types and perform OCR [35, 28, 37]. Focusing on image captioning only, LEMON [21] investigates scaling of an encoder-decoder model.

Several works have combined contrastive and captioning losses [64, 39, 33], optionally using a separate text encoder in addition to the decoder. While obtaining excellent results on a range of vision and vision-language tasks, the impact of the loss terms are not well disentangled, nor are compute-matched comparisons of individual losses provided.

Image captioning/alt-text prediction is a popular ingredient to build large multimodal models from separately pretrained vision and language models [1, 6, 60, 22, 17, 5]. Some of these models freeze large parts of vision and language components, sometimes only learning a small adapter between the two [1, 17, 38]. It is therefore interesting to see how the pretraining strategy for the vision model affects this type of adaption.

Finally, masked image-text modeling, often combined with image-text matching, is a popular pre-training strategy for encoder-only vision-language models at small data scale [23, 29, 40, 62, 54, 16].

3 A simple recipe to pretrain vision encoders via image captioning

Our goal is to establish a pretraining recipe based on image captioning that is comparable to CLIP in terms of simplicity, scalability, and efficiency. Therefore, we adopt Vision Transformer (ViT) [15] backbones as vision encoders, and use a standard Transformer decoder architecture [58] to predict image captions, feeding the ViT-encoded sequence to the decoder via cross-attention. As is common in recent literature [50, 11], we remove biases from attention layers, MLP blocks, and LayerNorms and we replace ReLU by GeLU. The decoder input and output embeddings are not shared. Ablations for these choices are in Section 4.4. The decoder has the same width, attention-heads, and MLP dimension as the encoder, but has half the depth. This leads to captioning models which have slightly lower parameter count than corresponding CLIP models, but require about the same pretraining compute in terms of accelerator hours per epoch (see Table 1). We rely on standard next-token-prediction language modeling and train our captioning models with causal attention mask and teacher forcing (Fig. 1, middle), henceforth referring to this variant simply as Captioner (Cap).

Parallel prediction We also experiment with a slightly modified training recipe (Fig. 1, right): Instead of training the model only for autoregressively, we train it to predict all tokens in parallel for a fraction of the training steps instead (alternating batches between the two prediction types throughout training). To this end, we replace the (shifted) decoder input sequence with a sequence of all [MASK] tokens, and drop the causal decoder attention mask. We emphasize that this kind of parallel prediction does not modify the training objective or decoder architecture, and does not incur any extra training cost, but simply modifies the decoder input sequence and attention mask for a fraction of training batches. Moreover, this is different from bag-of-word prediction as not only the presence but also the position of each token has to be predicted. We perform parallel prediction 75% of the training steps by default and term this variant Cap with parallel prediction (CapPa).

Intuitively, captioning via next token prediction induces an implicit weighting on the supervisory signal of the caption tokens: To predict the first few tokens of a caption, the decoder can benefit a lot from using the image information, while to predict later tokens it can rely more and more on already predicted tokens. Consequently, early tokens might provide a stronger supervisory signal to the encoder than later tokens. By contrast, when predicting all the caption tokens independently in parallel, the decoder can only rely on the image information to predict each token.

Implementation aspects We emphasize that our approach closely follows a standard encoder/decoder transformer architecture [58], with the only fundamental difference being the input data format and patch embedding, as well as the modification of the decoder input sequence and attention mask for parallel prediction. This means that our approach is easy to implement in existing transformer code bases [50, 45, 55]. We do not rely on image-specific preprocessing operations other than resizing, see Section 4.1. As a result, existing infrastructure for model-parallel and dis-

Table 2: Performance of frozen visual representations trained via image captioning (Cap/CapPa) and contrastively (CLIP*), when combined with a single transformer decoder trained from scratch for image classification, captioning and VQA (we use CIDEr for captioning, the VQAv2 weighted accuracy for VQAv2, and exact matching accuracy for all other tasks). Bold marks results where two standard-deviation interval overlaps with the two standard-deviation interval of the best result.

| | Classification | | | | | Captioning | | OCR | Question Ans. | |
|-------------|--------------------------------|--------------------------------|--------------------------------|--------------------------------|--------------------------------|---------------------------------|--------------------------------|--------------------------------|--------------------------------|--------------------------------|
| | i1k | sun | food | res | pet | COCO | Flickr | VQA | VQAv2 | GQA |
| Cap | 80.2 \pm 0.1 | 82.3 \pm 0.2 | 90.3 \pm 0.1 | 93.6 \pm 0.1 | 93.1 \pm 0.1 | 117.5\pm0.3 | 78.6\pm1.1 | 62.2\pm0.1 | 68.2\pm0.1 | 55.0 \pm 0.1 |
| CapPa | 81.3\pm0.1 | 82.4 \pm 0.1 | 90.9 \pm 0.1 | 94.2 \pm 0.2 | 94.4\pm0.1 | 117.9\pm0.6 | 80.5\pm0.2 | 62.2\pm0.0 | 68.3\pm0.1 | 55.7\pm0.2 |
| CLIP* (8k) | 81.1 \pm 0.0 | 83.2\pm0.1 | 91.2 \pm 0.0 | 94.8\pm0.0 | 93.4 \pm 0.2 | 115.8 \pm 0.2 | 74.5 \pm 1.2 | 56.0 \pm 0.1 | 66.5 \pm 0.1 | 54.3 \pm 0.3 |
| CLIP* (16k) | 81.4\pm0.1 | 83.3\pm0.1 | 92.0\pm0.1 | 95.2\pm0.2 | 93.6 \pm 0.2 | 116.3\pm0.7 | 77.1 \pm 0.7 | 56.5 \pm 0.1 | 66.7 \pm 0.1 | 54.8\pm0.6 |
| CLIP | 81.6 \pm 0.1 | 82.5 \pm 0.0 | 92.6 \pm 0.1 | 94.9 \pm 0.1 | 93.6 \pm 0.1 | 118.4 \pm 0.6 | 78.7 \pm 0.9 | 60.0 \pm 0.1 | 67.8 \pm 0.1 | 57.5 \pm 0.1 |
| CapPa L/14 | 84.4 \pm 0.0 | 84.9 \pm 0.1 | 93.8 \pm 0.0 | 96.0 \pm 0.1 | 95.6\pm0.0 | 125.8\pm0.1 | 89.3\pm1.4 | 65.6\pm0.1 | 70.9\pm0.0 | 58.3\pm0.2 |
| CLIP* L/14 | 84.7\pm0.1 | 85.7\pm0.1 | 94.6\pm0.1 | 96.4\pm0.0 | 95.2 \pm 0.1 | 123.2 \pm 0.6 | 85.5 \pm 0.3 | 61.3 \pm 0.2 | 68.5 \pm 0.1 | 55.3 \pm 0.1 |
| CLIP L/14 | 84.8 \pm 0.0 | 84.8 \pm 0.1 | 95.2 \pm 0.1 | 96.3 \pm 0.1 | 95.4 \pm 0.3 | 124.4 \pm 0.6 | 87.1 \pm 0.7 | 64.1 \pm 0.0 | 70.4 \pm 0.1 | 58.7 \pm 0.1 |

tributed training can readily be used to scale our approach. In particular, our loss does not require computations across devices the way CLIP does.

Zero-shot classification via scoring Image captioning models allow for zero-shot classification simply by scoring the class name. Unlike with contrastive models, where the text (class) embeddings can be computed once and reused for new images, with captioning models all class names have to be scored again for every new image. Cap/CapPa are hence less efficient zero-shot classifiers than CLIP. We emphasize that we focus on learning vision encoders here and zero-shot transfer is not our focus.

4 Experiments

4.1 Experiment setup

Pretraining data We use a subset of the WebLI data set [6] which contains 10B images and 12B multilingual alt-texts. Specifically, we rely on the WebLI subset corresponding to English websites and apply text-based filtering similar to [25, Sec. 3], [4, Sec 2.2] to obtain 1B image/alt-text pairs, not using any image-text similarity-based filtering. Importantly, WebLI was de-duplicated w.r.t. the images in the evaluation data sets we use in this paper. Please refer to [6, Sec 2.2] for more details on the WebLI data set and to [6, Appendix B] for a datasheet.

Table 1: Parameter count and TPUv4-hrs. per bn. examples seen.

| Model | Params | TPU-hrs. |
|------------|--------|----------|
| B/16 Cap | 192 M | 454 |
| B/16 CLIP* | 197 M | 444 |
| L/14 Cap | 570 M | 1570 |
| L/14 CLIP* | 640 M | 1596 |

Pretraining details and baselines We use a batch size of 8k for our captioning models (larger batch size did not lead to improved performance), and both 8k and 16k for our retrained CLIP baselines (henceforth denoted by CLIP* to avoid confusion with the model checkpoints released by [48], which we reference by CLIP in our results). We explicitly note the batch size for CLIP* models when relevant; CLIP* without modifier refers to the variant trained with batch size 16k. Models are trained on up to 9B image/alt-text pairs (corresponding to 9 epochs on our subset of WebLI). We use the AdaFactor variant from [66] with a cosine schedule (with 10k warmup steps), and set learning rate and decay factor to 10^{-3} and 10^{-4} , respectively. Previous work [68, 67, 57] established these optimizer settings for contrastive pretraining and we adopt them here for captioning. Images are resized to a resolution of 224×224 , and alt-texts are tokenized to a 32k-sized vocabulary with a sentence piece model trained on the English portion of C4 [50], with a maximum sequence length of 64. Following [68, 67, 57] for CLIP* we use identically sized image and text towers, and use global average pooling (GAP) to compute the image representation.

Table 3: 10-shot linear evaluation accuracy on the pre-logit representation. CapPa outperforms Cap and achieves overall comparable results with CLIP* trained with a batch size of 16k.

| | INet | CIFAR100 | Pets | Cars |
|-------------|----------------------------------|----------------------------------|----------------------------------|----------------------------------|
| Cap | 57.2 ± 0.1 | 58.6 ± 0.8 | 83.7 ± 0.6 | 84.2 ± 0.1 |
| CapPa | 59.1 ± 0.1 | 62.4 ± 0.4 | 86.5 ± 0.1 | 86.6 ± 0.2 |
| CLIP* (8k) | 58.5 ± 0.1 | 64.9 ± 0.4 | 77.7 ± 1.5 | 80.8 ± 0.4 |
| CLIP* (16k) | 59.7 ± 0.4 | 66.3 ± 0.2 | 80.6 ± 1.2 | 82.9 ± 0.1 |
| CLIP | 59.0 ± 0.2 | 68.6 ± 0.1 | 82.1 ± 0.7 | 70.2 ± 0.7 |
| CapPa L/14 | 70.6 ± 0.2 | 72.9 ± 0.4 | 92.6 ± 0.5 | 92.2 ± 0.2 |
| CLIP* L/14 | 69.8 ± 0.1 | 74.1 ± 0.5 | 87.7 ± 0.9 | 89.2 ± 0.2 |
| CLIP L/14 | 69.7 ± 0.1 | 79.4 ± 0.3 | 90.4 ± 0.8 | 81.1 ± 0.4 |

Table 4: Frozen transfer for zero-shot classification and retrieval via LiT [68]. Especially for the larger model, CapPa is competitive with CLIP* with comparable or fewer LiT examples seen.

| LiT pairs: | INet 0shot | | COCO t2i | | COCO i2t | |
|------------|------------|-------------|----------|-------------|----------|-------------|
| | 3B | 12B | 3B | 12B | 3B | 12B |
| Cap | 67.8 | 69.0 | 37.5 | 39.1 | 53.9 | 54.8 |
| CapPa | 68.8 | 70.2 | 37.3 | 38.6 | 53.9 | 55.1 |
| CLIP* | 69.0 | 70.0 | 38.9 | 40.1 | 55.1 | 57.0 |
| CLIP | | 68.3 | | 32.3 | | 52.8 |
| CapPa L/14 | 76.4 | 77.5 | 43.9 | 45.4 | 60.3 | 62.6 |
| CLIP* L/14 | 75.8 | 76.6 | 44.7 | 46.3 | 60.7 | 62.3 |
| CLIP L/14 | | 75.1 | | 36.5 | | 56.6 |

4.2 Evaluation protocols and data sets

We focus on properties of the frozen representations and also present some fine-tuning results.

Probing the frozen representation As an inexpensive way to assess classification performance we use the linear adaptation protocol (based on the pre-logits layer for CLIP* and GAP of the encoder output sequence for our captioning models) and eval sets from [66, 68], reporting the 10-shot classification accuracy. We also evaluate the classification accuracy when using the full ImageNet1k training set to learn a dense layer, an MLP, and a multihead attention pooling (MAP)-based [34] classifier. To assess the amenability of the different the CLIP* and CapPa vision encoders to fine-grained classification, we train MAP-based classifiers on a range of specialized data sets which can be divided in two groups. The first group requires fine-grained classification of animal or plant breed [43, 59, 46, 27], or product variant [31, 3], whereas data sets in the second group covers a range of distinct objects [18, 12, 8, 69, 44, 19].

Text encoder/decoder-based inference We use LiT [68] to learn a text embedding matched to the embedding of our pretrained vision encoders. Generally, LiT is an efficient way to equip any pretrained vision backbone with zero-shot classification and retrieval capabilities, here particularly for Cap whose pretrained decoder does in principle have these capabilities but incurs significant inference cost. We follow the setup from [67] and assess the zero-shot classification accuracy on ImageNet1k [51] and retrieval recall@1 on COCO captions [7]. We choose the LiT text encoder to mirror the architecture of the vision encoder at hand and attach a randomly initialized MAP head to the vision encoder to map into the shared image-text embedding space. For comparison, we also apply LiT to our CLIP* models; this is not necessarily meant to be practically useful (continuing training the CLIP* model might be a better investment of compute).

Motivated by recent work combining pretrained vision backbones and language models [1, 6, 60, 22, 17, 5], we investigate the amenability of the learned representations to interface with a text decoder. Concretely, we use the “LiT decoder” setup [2] which trains a transformer decoder from scratch on top of a frozen vision representation to solve captioning [7, 63], VQA [20, 24, 41] and classification [51, 69, 3, 8, 46] tasks in a multitask fashion (we use the default hyperparameters from [2] except for the data mixing strategy set to “concat image-question pairs” [2, Sec. 5.3]).

In addition, we explore combining our representations with a pretrained T5 decoder [50]. We rely on the previously described multitask LiT decoder setup and tune the most important hyper parameters (see supplementary material for details). For the T5 decoder we keep all the parameters frozen but reinitialize and train the cross-attention layers. Finally, we also leverage a frozen, pretrained 12-layer GPT-2 decoder [49] for image captioning by combining it with the frozen vision encoders via an adapter, similar to ClipCap [42].

Fine-tuning We fine-tune our vision encoders on the full ImageNet1k data set, attaching a randomly initialized MAP head to the pretrained representation (see supplementary material for details).

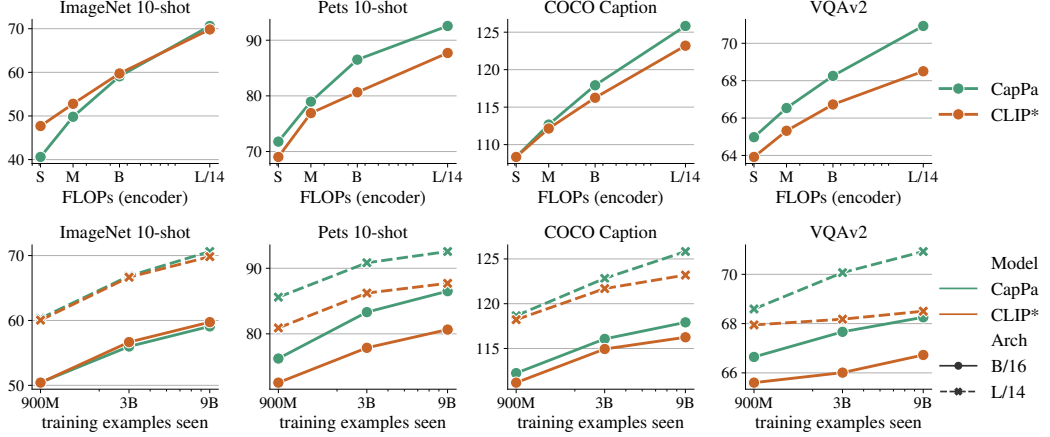


Figure 2: 10-shot classification accuracy on the frozen pre-logit representation (left two columns); captioning and VQA performance with a decoder (right two columns). **Top row:** Performance of vision backbones pretrained with captioning (Cap/CapPa) and contrastively (CLIP*) as a function of the model size/FLOPs (we compare ViT-S/16, M/16, B/16, and L/14). CapPa exhibits favorable scaling behavior on captioning and VQA tasks. **Bottom row:** Performance of CapPa and CLIP* as a function of the number of training examples seen. The behavior is similar as for model scale.

Using the pretrained text decoder Finally, we also evaluate our models (with the pretrained text decoder) on the Attribute, Relation and Order (ARO) benchmark [65], which is derived from the captioning test sets of Visual Genome [32], Flickr-30K [63] and COCO captions [7]. Specifically, ARO shuffles the attributes, relations and order of captions and measures the sensitivity of vision-language models to these manipulations. As shown by [65], contrastive models are not very sensitive to precise relational and attributional information and behave closer to bag-of-words models. Intuitively, since captioning-based models model the joint distribution over all tokens, it is interesting to see how they compare to contrastive models on ARO. For each example, we use log-likelihood to score both the true caption and the shuffled captions. The model prediction is the caption with the highest score.

4.3 Main results

Tables 2, 3, 4, and Fig. 3 show the LiT decoder results, the 10-shot classification accuracy, the LiT tuning results, and the full linear probing accuracy for our models trained for 9B examples seen.

CapPa outperforms Cap across almost all evaluations, and often also outperforms CLIP* trained with the same batch size (8k), while being competitive with CLIP* trained with a batch size of 16k. This is remarkable since CLIP* benefits substantially from a large batch size [67]. The trend becomes more pronounced when increasing the model size: CapPa clearly outperforms CLIP* in 10-shot classification accuracy for a ViT-L/14 encoder (Table 3).

When transferred to ImageNet1k classification with a linear probe (Fig. 3), the frozen Cap and CapPa encoders lag somewhat behind CLIP*, but the gap almost vanishes when using a MAP head instead of a linear probe. This is not very surprising, given CLIP* models are trained with a linear head, which might induce linear separability in the average pooled encoder output representation. In contrast, the Cap models feed into a decoder via cross-attention which might not impose linear separability as strongly. For fine-tuning the full model on ImageNet1k (Table 5) we only observe a minor gap between CapPa and CLIP*. As for text encoders learned via LiT (Table 4) CapPa outperforms CLIP* for long LiT training and large model size in zero-shot classification, but is outperformed by CLIP* in retrieval. Notably, for a short LiT tuning with 3B examples our models outperform CLIP [48] in zero-shot classification and retrieval while matching the number of training examples seen by CLIP (12.8B) when summing over pretraining (9B) and LiT tuning (3B), despite the vision encoder being frozen during LiT tuning (which saves compute). Matching the number of examples seen by CLIP during LiT tuning (12B) leads to a clear additional improvement.

Table 5: Finetuning on INet.

| | B/16 | B/16 ₃₈₄ | L/14 ₃₃₆ |
|-------|------|---------------------|---------------------|
| CLIP* | 84.9 | 86.0 | 88.1 |
| CapPa | 84.4 | 85.7 | 87.7 |
| Cap | 83.9 | 85.3 | - |

| | Attrib. | Rel. | Order (F) | Order (C) |
|------------|---------|------|-----------|-----------|
| Blind dec. | 83.7 | 86.2 | 98.8 | 98.7 |
| Cap | 88.9 | 86.6 | 99.1 | 99.0 |
| CapPa | 85.7 | 86.7 | 99.2 | 98.8 |
| CLIP* | 53.2 | 39.7 | 45.5 | 37.0 |
| CLIP | 62.7 | 58.7 | 57.9 | 49.5 |
| ARO Best | 88.0 | 73.0 | 60.0 | 46.0 |
| NegCLIP | 71.0 | 81.0 | 91.0 | 86.0 |

Table 6: Results on the Attribute, Relation and Order (ARO) benchmark [65]. Cap and CapPa clearly outperform all CLIP* and CLIP variants across all data sets. They also outperform NegCLIP [65] which was explicitly trained to be sensitive to word ordering and attribution.

Combining our models with a fresh (LiT) decoder (Table 2), we observe that CapPa performs better than CLIP* trained with batch size 16k on captioning and VQA, while obtaining competitive accuracy on classification tasks. Again, this pattern becomes more pronounced with increased models size. Indeed, for a ViT-L/14 encoder CapPa even outperforms CLIP in the majority of LiT decoder tasks.

Scaling properties In Fig. 2 we present an analysis of our encoders as a function of the model size and the number of training examples seen for a selection of 10-shot classification and vision & language evaluations using a fresh decoder (plots for all evaluations and Cap can be found in the supplementary material). It can be seen that CLIP* and CapPa models exhibit similar scaling behavior, with CapPa showing a somewhat steeper increase in captioning and VQA performance as a function of model size and examples seen, in particular for a ViT-L/14 backbone. This indicates that the benefits of CapPa models might become more pronounced with further model and data scaling.

Attribution, relation, ordering Table 6 presents our results on the ARO Benchmark [65]. Cap and CapPa models achieve close to a perfect score on the ordering subsets. They outperform the best contrastive variants by around 30% and 40% on Flickr Order and COCO Order, respectively. We also compare with NegCLIP [65], which employs additional supervision to make contrastive models sensitive to word ordering and attribution. Cap and CapPa exceed NegCLIP by 8% and 13% out-of-the-box on COCO Order and Flickr Order. The same can be observed for the attribution, and relation subsets of ARO. So we are facing a clear trade-off: CLIP-style models outperform captioning-based models in terms of standard zero-shot classification accuracy, whereas the latter are much better at processing fine-grained descriptions of visual content. Finally, we also trained a Cap model with no image input (Blind dec.), which is just a language model for alt-text. This model overall performs only slightly worse than Cap and CapPa, which suggests that the sentence manipulation in ARO can to a large extent be detected by language modeling alone.

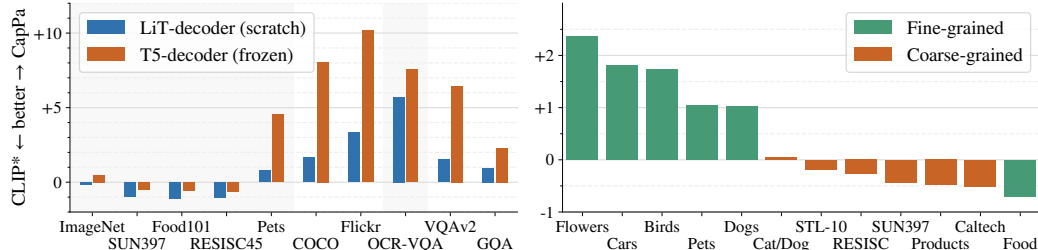


Figure 4: Absolute improvement of CapPa over CLIP* in various settings. **Left:** CapPa pairs significantly better with decoders in image-language tasks, especially when the decoder is a pre-trained and frozen language model. **Right:** CapPa seems to be a noticeably better frozen feature extractor for fine-grained classification tasks (we show L/14 results, see appendix for B/16).

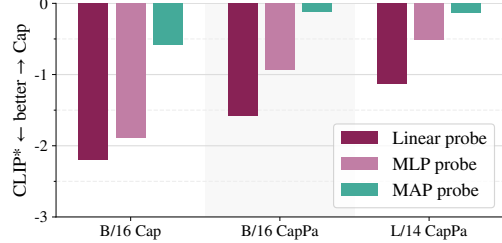


Figure 3: While linear probes give the impression that captioning leads to worse feature extractors, using a Multihead Attention Pooling (MAP) probe instead essentially closes the gap. The extracted features are hence equally informative, but pooling them correctly needs to be learned.

Table 7: Impact of decoder architecture design choices in Cap on 10-shot linear classification accuracy: **Left:** Effect of sharing the embedding between decoder input and output and removing biases from decoder layers. **Right:** Effect of the number of decoder layers.

| share emb. | dec. bias | ImageNet | CIFAR100 | Pets | Cars | dec. layers | ImageNet | CIFAR100 | Pets | Cars |
|------------|-----------|----------|----------|------|------|-------------|----------|----------|------|------|
| yes | no | 47.8 | 55.8 | 71.5 | 71.7 | 3 | 48.7 | 53.7 | 73.5 | 73.7 |
| no | no | 49.7 | 56.0 | 72.6 | 74.7 | 6 | 49.7 | 56.0 | 72.6 | 74.7 |
| yes | yes | 48.3 | 54.6 | 74.4 | 70.2 | 12 | 48.7 | 54.8 | 74.4 | 73.8 |
| no | yes | 49.3 | 56.6 | 72.7 | 71.9 | | | | | |

Frozen T5 decoder We also trained models with frozen encoder *and* frozen decoder (initialized with a T5 checkpoint). For these experiments, only the cross attention weights were trained (28M trainable parameters, compared to the 248M trainable parameters when the decoder is trained from scratch). The relative improvements of CapPa over CLIP* are shown in Fig. 4 (left). Even though the absolute performance of the decoder trained from scratch (Table 2) is better than when only training the cross attention weights (Table 11), CapPa with a frozen decoder closes the gap on three classification tasks, reverts the trend on ImageNet, and improves the performance by large margins on Pets, as well as all captioning and VQA tasks. This result suggests that the captioning objective is better suited to train an encoder that is later combined with a pretrained language decoder.

Frozen GPT-2 decoder We combined our frozen vision encoders with a frozen GPT-2 model from [49] using an adapter as proposed by ClipCap [42]. We found that this setup is less well suited for VQA and multitask conditioning, so we only evaluate it on captioning in single-task fashion as done by ClipCap. We tried the MLP and transformer adapters from [42], but obtained better results for both CLIP* and CapPa with a “resampler”, a LayerNorm followed by a single cross-attention layer with learnable query embeddings, generating a prefix of 32 soft tokens for GPT-2. This resampler has only 7.1M parameters, about 4× less than the MLP adapter from [42]. CapPa still outperforms CLIP* in this setup, but the gains are more modest than for the T5 decoder and a decoder trained from scratch (both single-task, see Fig. 5). We emphasize that both encoder and GPT-2 decoder are frozen and we only use a small adapter.

Fine-grained classification Fig. 4 (right) shows the improvement when using CapPa instead of CLIP* for a range of specialized data sets. CapPa outperforms CLIP* on the majority of fine-grained tasks which suggests that captioning as a pretraining task leads to better features for fine-grained classification than contrastive pretraining.

4.4 Ablations

All models discussed in this section are trained for 900M training examples seen.

Decoder architecture While following the original transformer decoder architecture [58] closely, we investigate several modifications that have become common in the literature [50, 11]. Specifically, we ablate the effect of removing biases in decoder layers, as well as sharing the decoder input and output embeddings. Table 7 (left) shows that not sharing the embeddings leads to overall better 10-shot accuracy than sharing them, and additionally removing the decoder biases does not hurt. Furthermore, we observed significantly improved stability across encoder architectures, scales and training schedules when removing the decoder biases.

Table 7 (right) reveals that the overall best 10-shot classification accuracy is obtained when using a 6 layer decoder. This decoder depth also leads to a total parameter count comparable to the corresponding CLIP* model (Table 1).

Inspired by experiments from [66], where applying a stronger weight decay to the classification head of ViTs trained for image classification led to accuracy improvements, we also experimented with

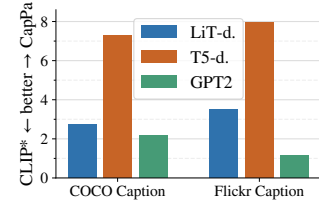


Figure 5: Absolute improvement (single-task) of CapPa over CLIP* for a decoder trained from scratch (LiT-d.), a frozen T5 decoder, and a frozen GPT-2 similar to [42].

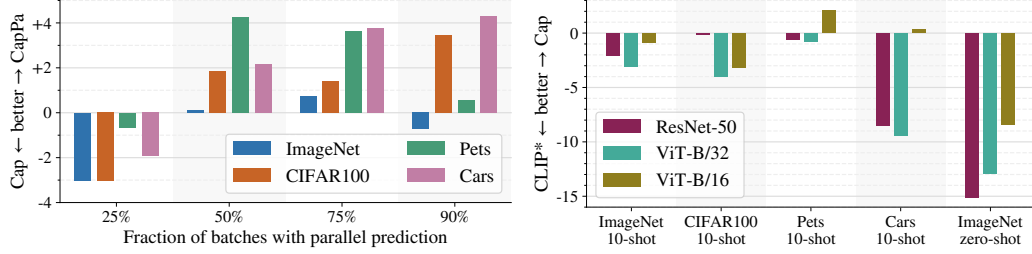


Figure 7: **Left:** Improvement in 10-shot classification accuracy as a function of the fraction of training batches for which parallel prediction is performed in CapPa. A fraction of 0.75 leads to a balanced improvement. **Right:** Improvement of 10-shot/zero-shot (without prompts) classification accuracy when using Cap instead of CLIP*. Cap is competitive in 10-shot accuracy for ViT-B/16.

increased weight decay applied to the decoder or cross-attention layers, but we did not observe any benefits from this. Further, we explored using a tokenizer trained on 300M randomly sampled WebLI alt-texts instead of the one pretrained on C4, which did not improve accuracy.

Parallel prediction Recall that for parallel prediction we replace all text input tokens with [MASK] tokens. An alternative would be to only replace a random subset, as done e.g. in [21], to provide a partial context for the prediction. However, we did not observe improvements of the vision encoder when only masking a fraction of the tokens, so we focused on fully masked input sequences. For fully masked input sequence Fig. 7 (left) shows the improvement in 10-shot classification accuracy over training for pure autoregressive decoding as a function of the fraction of batches for which the decoder is trained for parallel prediction instead. A fraction of 0.75 leads to a balanced improvement across all considered data sets. Finally, performing parallel prediction with mixed batches, rather than alternating between parallel and autoregressive prediction for all examples in a batch led to significantly worse results.

Encoder architecture Next, we investigate the effect of the encoder architecture on the representation quality, comparing CLIP* with Cap when using a BiT ResNet50 [30], ViT-B/32, and a ViT B/16 vision encoder (we use a B-sized text encoder and B-sized 6-layer decoder for CLIP* and Cap, respectively, for all encoders). According to [15] the BiT ResNet50 obtains performance roughly comparable to ViT-B/32 when trained and evaluated on image classification. Further, ResNet50 and ViT-B/32 both produce a sequence of length 49 before pooling for 224×224 images, which we feed to the decoder. Fig. 7 (right) shows the improvement obtained when using Cap instead of CLIP* as a function of the encoder architecture. The improvement (regression) in ImageNet zero-shot accuracy is smallest (largest) for the ResNet50 architecture (this is the architecture used to create [48, Fig. 2] that compares contrastive with bag-of-words and captioning approaches) and is significantly improved when using a ViT architecture and when reducing the patch size (which does not increase model capacity but the sequence length and hence FLOPs). Also recall that these models were only trained on 900M examples. Interestingly, the difference between CLIP* and Cap on 10-shot metrics are generally smaller, and for a ViT-B/16 encoder the two approaches lead to similar performance.

Effect of pretraining data So far all our results were based on models pretrained on a variant of WebLI, and one might wonder whether our findings transfer to pre-training on other data sets. We therefore train some of our models and baselines on the smaller, publicly available LAION-400M dataset [53] which was collected and filtered following a different protocol. For instance, it was filtered using an existing CLIP model to score image-text pairs, which might induce a significantly different bias in the training data and our conclusions. However, the 10-shot linear classification results in Fig. 6 show that the conclusions remain the same: CapPa achieves accuracy comparable with CLIP* and outperforms Cap.

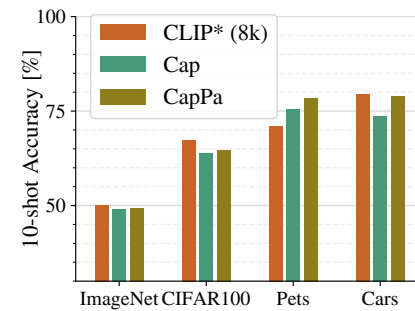


Figure 6: Pretraining on LAION-400M.

5 Discussion and conclusion

We presented an extensive comparison of vision encoders pretrained with a contrastive and generative (captioning) objective and found that the generatively pretrained encoders obtain better performance when used for captioning, VQA, fine-grained and few-shot classification tasks, while achieving competitive performance in classification overall. This is in contrast to previous work [48] which argued that predicting alt-text from images *explicitly and exactly* is an overly challenging pretraining task and may lead to sub-par vision capabilities. Moreover, our results show that captioning as a pretraining task might exhibit favorable scaling properties with increasing model and data scale, and we hope future work will explore this avenue.

One downside of our approach is that the Cap/CapPa text decoder is of limited use. While it achieves excellent results when word order and object relationships matter—a scenario where CLIP-style models exhibit a strong bag-of-word bias—zero-shot classification and retrieval are computationally expensive. We showed that this can be mitigated relatively cheaply by training a text encoder matched to the frozen Cap/CapPa representation via LiT tuning. Note that such a procedure is significantly cheaper than training the text encoder with the image encoder and text decoder throughout the whole pretraining procedure as done e.g. by CoCa [64]. Another promising avenue is to explore parallel prediction for inference task, as it would allow for efficient scoring e.g. for zero-shot classification. Indeed, parallel prediction produces a joint distribution over all tokens, which can be used to score an arbitrary number of classes or queries.

In conclusion, we established plain image captioning as a competitive pretraining strategy for vision backbones from image-text data. We hope to inspire follow up work dedicating more attention the advantages of captioning as a pretraining task for vision encoders.

Acknowledgments We would like to thank Jannis Bulian, Mostafa Dehghani, Alexey Dosovitskiy, Daniel Keysers, Mario Lucic, Basil Mustafa, and Xiao Wang for feedback on this paper and inspiring discussions on captioning-based pretraining. We would also like to thank Janko Ferlić from Unsplash for providing the photo used in Fig. 1.

References

- [1] Jean-Baptiste Alayrac, Jeff Donahue, Pauline Luc, Antoine Miech, Iain Barr, Yana Hasson, Karel Lenc, Arthur Mensch, Katie Millican, Malcolm Reynolds, Roman Ring, Eliza Rutherford, Serkan Cabi, Tengda Han, Zhitao Gong, Sina Samangooei, Marianne Monteiro, Jacob Menick, Sebastian Borgeaud, Andrew Brock, Aida Nematzadeh, Sahand Sharifzadeh, Mikolaj Binkowski, Ricardo Barreira, Oriol Vinyals, Andrew Zisserman, and Karen Simonyan. Flamingo: A visual language model for few-shot learning. In *NeurIPS*, 2022. [1](#), [2](#), [3](#), [5](#)
- [2] Lucas Beyer, Bo Wan, Gagan Madan, Filip Pavetic, Andreas Steiner, Alexander Kolesnikov, André Susano Pinto, Emanuele Bugliarello, Xiao Wang, Qihang Yu, Liang-Chieh Chen, and Xiaohua Zhai. A study of autoregressive decoders for multi-tasking in computer vision. *arXiv:2303.17376*, 2023. [5](#), [15](#), [18](#), [19](#), [21](#)
- [3] Lukas Bossard, Matthieu Guillaumin, and Luc Van Gool. Food-101 – mining discriminative components with random forests. In *ECCV*, 2014. [5](#), [17](#)
- [4] Soravit Changpinyo, Piyush Sharma, Nan Ding, and Radu Soricut. Conceptual 12M: Pushing web-scale image-text pre-training to recognize long-tail visual concepts. In *CVPR*, 2021. [4](#)
- [5] Xi Chen, Josip Djolonga, Piotr Padlewski, Basil Mustafa, Soravit Changpinyo, Jialin Wu, Carlos Riquelme Ruiz, Sebastian Goodman, Xiao Wang, Yi Tay, Siamak Shakeri, Mostafa Dehghani, Daniel Salz, Mario Lucic, Michael Tschannen, Arsha Nagrani, Hexiang Hu, Mandar Joshi, Bo Pang, Ceslee Montgomery, Paulina Pietrzyk, Marvin Ritter, AJ Piergiovanni, Matthias Minderer, Filip Pavetic, Austin Waters, Gang Li, Ibrahim Alabdulmohsin, Lucas Beyer, Julien Amelot, Kenton Lee, Andreas Peter Steiner, Yang Li, Daniel Keysers, Anurag Arnab, Yuanzhong Xu, Keran Rong, Alexander Kolesnikov, Mojtaba Seyedhosseini, Anelia Angelova, Xiaohua Zhai, Neil Houlsby, and Radu Soricut. PaLI-X: On scaling up a multilingual vision and language model. *arXiv:2305.18565*, 2023. [1](#), [2](#), [3](#), [5](#)
- [6] Xi Chen, Xiao Wang, Soravit Changpinyo, A. J. Piergiovanni, Piotr Padlewski, Daniel Salz, Sebastian Goodman, Adam Grycner, Basil Mustafa, Lucas Beyer, Alexander Kolesnikov, Joan Puigcerver, Nan Ding, Keran Rong, Hassan Akbari, Gaurav Mishra, Linting Xue, Ashish Thapliyal, James Bradbury, Weicheng Kuo, Mojtaba Seyedhosseini, Chao Jia, Burcu Karagol Ayan, Carlos Riquelme, Andreas Steiner, Anelia Angelova, Xiaohua Zhai, Neil Houlsby, and Radu Soricut. PaLI: A jointly-scaled multilingual language-image model. In *ICLR*, 2023. [1](#), [2](#), [3](#), [4](#), [5](#)
- [7] Xinlei Chen, Hao Fang, Tsung-Yi Lin, Ramakrishna Vedantam, Saurabh Gupta, Piotr Dollár, and C. Lawrence Zitnick. Microsoft COCO Captions: Data collection and evaluation server. *arXiv preprint arXiv:1504.00325*, 2015. [5](#), [6](#)
- [8] Gong Cheng, Junwei Han, and Xiaoqiang Lu. Remote sensing image scene classification: Benchmark and state of the art. *arXiv preprint arXiv:1703.00121*, 2017. [5](#), [17](#)
- [9] Mehdi Cherti, Romain Beaumont, Ross Wightman, Mitchell Wortsman, Gabriel Ilharco, Cade Gordon, Christoph Schuhmann, Ludwig Schmidt, and Jenia Jitsev. Reproducible scaling laws for contrastive language-image learning. In *CVPR*, pages 2818–2829, 2023. [1](#)
- [10] Jaemin Cho, Jie Lei, Hao Tan, and Mohit Bansal. Unifying vision-and-language tasks via text generation. In *ICML*, pages 1931–1942, 2021. [1](#)
- [11] Aakanksha Chowdhery, Sharan Narang, Jacob Devlin, Maarten Bosma, Gaurav Mishra, Adam Roberts, Paul Barham, Hyung Won Chung, Charles Sutton, Sebastian Gehrmann, Parker Schuh, Kensen Shi, Sasha Tsvyashchenko, Joshua Maynez, Abhishek Rao, Parker Barnes, Yi Tay, Noam Shazeer, Vinodkumar Prabhakaran, Emily Reif, Nan Du, Ben Hutchinson, Reiner Pope, James Bradbury, Jacob Austin, Michael Isard, Guy Gur-Ari, Pengcheng Yin, Toju Duke, Anselm Levskaya, Sanjay Ghemawat, Sunipa Dev, Henryk Michalewski, Xavier Garcia, Vedant Misra, Kevin Robinson, Liam Fedus, Denny Zhou, Daphne Ippolito, David Luan, Hyeontaek Lim, Barret Zoph, Alexander Spiridonov, Ryan Sepassi, David Dohan, Shivani Agrawal, Mark Omernick, Andrew M. Dai, Thanumalayan Sankaranarayana Pillai, Marie Pellat, Aitor Lewkowycz, Erica Moreira, Rewon Child, Oleksandr Polozov, Katherine Lee, Zongwei Zhou, Xuezhi Wang, Brennan Saeta, Mark Diaz, Orhan Firat, Michele Catasta, Jason Wei, Kathy Meier-Hellstern, Douglas Eck, Jeff Dean, Slav Petrov, and Noah Fiedel. PaLM: Scaling language modeling with pathways. *arXiv:2204.02311*, 2022. [3](#), [8](#)
- [12] Adam Coates, Andrew Ng, and Honglak Lee. An analysis of single-layer networks in unsupervised feature learning. In *AISTATS*, pages 215–223, 2011. [5](#), [17](#)
- [13] Karan Desai and Justin Johnson. VirTex: Learning visual representations from textual annotations. In *CVPR*, 2021. [1](#), [2](#)

[14] Xiaoyi Dong, Jianmin Bao, Ting Zhang, Dongdong Chen, Shuyang Gu, Weiming Zhang, Lu Yuan, Dong Chen, Fang Wen, and Nenghai Yu. CLIP Itself is a Strong Fine-tuner: Achieving 85.7% and 88.0% Top-1 Accuracy with ViT-B and ViT-L on ImageNet. *arXiv:2212.06138*, 2022. 1, 15

[15] Alexey Dosovitskiy, Lucas Beyer, Alexander Kolesnikov, Dirk Weissenborn, Xiaohua Zhai, Thomas Unterthiner, Mostafa Dehghani, Matthias Minderer, Georg Heigold, Sylvain Gelly, Jakob Uszkoreit, and Neil Houlsby. An image is worth 16×16 words: Transformers for image recognition at scale. In *ICLR*, 2021. 1, 3, 9, 15

[16] Zi-Yi Dou, Yichong Xu, Zhe Gan, Jianfeng Wang, Shuohang Wang, Lijuan Wang, Chenguang Zhu, Pengchuan Zhang, Lu Yuan, Nanyun Peng, Zicheng Liu, and Michael Zeng. An empirical study of training end-to-end vision-and-language transformers. In *CVPR*, pages 18145–18155, 2022. 3

[17] Danny Driess, F. Xia, Mehdi S. M. Sajjadi, Corey Lynch, Aakanksha Chowdhery, Brian Ichter, Ayzaan Wahid, Jonathan Tompson, Quan Ho Vuong, Tianhe Yu, Wenlong Huang, Yevgen Chebotar, Pierre Sermanet, Daniel Duckworth, Sergey Levine, Vincent Vanhoucke, Karol Hausman, Marc Toussaint, Klaus Greff, Andy Zeng, Igor Mordatch, and Peter R. Florence. Palm-E: An embodied multimodal language model. *arXiv:2303.03378*, 2023. 1, 2, 3, 5

[18] Jeremy Elson, John R. Douceur, Jon Howell, and Jared Saul. Asirra: A CAPTCHA that Exploits Interest-Aligned Manual Image Categorization. In *Proc. ACM Conf. Computer and Communications Security (CCS)*, 2007. 5, 17

[19] Li Fei-Fei, Rob Fergus, and Pietro Perona. Learning generative visual models from few training examples: An incremental bayesian approach tested on 101 object categories. In *CVPRW*, pages 178–178, 2004. 5, 17

[20] Yash Goyal, Tejas Khot, Douglas Summers-Stay, Dhruv Batra, and Devi Parikh. Making the V in VQA matter: Elevating the role of image understanding in visual question answering. In *CVPR*, 2017. 5

[21] Xiaowei Hu, Zhe Gan, Jianfeng Wang, Zhengyuan Yang, Zicheng Liu, Yumao Lu, and Lijuan Wang. Scaling up vision-language pre-training for image captioning. In *CVPR*, pages 17980–17989, 2022. 1, 3, 9

[22] Shaohan Huang, Li Dong, Wenhui Wang, Yaru Hao, Saksham Singhal, Shuming Ma, Tengchao Lv, Lei Cui, Owais Khan Mohammed, Qiang Liu, Kriti Aggarwal, Zewen Chi, Johan BJORCK, Vishrav Chaudhary, Subhajit Som, Xia Song, and Furu Wei. Language is not all you need: Aligning perception with language models. *arXiv:2302.14045*, 2023. 1, 2, 3, 5

[23] Zhicheng Huang, Zhaoyang Zeng, Bei Liu, Dongmei Fu, and Jianlong Fu. Pixel-BERT: Aligning image pixels with text by deep multi-modal transformers. *arXiv:2004.00849*, 2020. 3

[24] Drew A. Hudson and Christopher D. Manning. GQA: a new dataset for compositional question answering over real-world images. In *CVPR*, 2019. 5

[25] Chao Jia, Yinfei Yang, Ye Xia, Yi-Ting Chen, Zarana Parekh, Hieu Pham, Quoc V. Le, Yun-Hsuan Sung, Zhen Li, and Tom Duerig. Scaling up visual and vision-language representation learning with noisy text supervision. In *ICML*, 2021. 1, 2, 4

[26] Armand Joulin, Laurens Van Der Maaten, Allan Jabri, and Nicolas Vasilache. Learning visual features from large weakly supervised data. In *ECCV*, pages 67–84, 2016. 1, 2

[27] Aditya Khosla, Nityananda Jayadevaprakash, Bangpeng Yao, and Fei-Fei Li. Novel dataset for fine-grained image categorization: Stanford dogs. In *CVPRW*, 2011. 5, 17

[28] Geewook Kim, Teakgyu Hong, Moonbin Yim, JeongYeon Nam, Jinyoung Park, Jinyeong Yim, Won-seok Hwang, Sangdoo Yun, Dongyo Han, and Seunghyun Park. OCR-Free document understanding transformer. In *ECCV*, pages 498–517, 2022. 3

[29] Wonjae Kim, Bokyung Son, and Ildoo Kim. ViLT: Vision-and-language transformer without convolution or region supervision. In *ICML*, pages 5583–5594. PMLR, 2021. 3

[30] Alexander Kolesnikov, Lucas Beyer, Xiaohua Zhai, Joan Puigcerver, Jessica Yung, Sylvain Gelly, and Neil Houlsby. Big transfer (BiT): General visual representation learning. In *ECCV*, 2020. 9

[31] Jonathan Krause, Michael Stark, Jia Deng, and Li Fei-Fei. 3d object representations for fine-grained categorization. In *CVPRW*, pages 554–561, 2013. 5, 17

[32] Ranjay Krishna, Yuke Zhu, Oliver Groth, Justin Johnson, Kenji Hata, Joshua Kravitz, Stephanie Chen, Yannis Kalantidis, Li-Jia Li, David A Shamma, et al. Visual genome: Connecting language and vision using crowdsourced dense image annotations. *IJCV*, pages 32–73, 2017. 6

[33] Weicheng Kuo, AJ Piergiovanni, Dahun Kim, Xiyang Luo, Ben Caine, Wei Li, Abhijit Ogale, Luowei Zhou, Andrew Dai, Zhifeng Chen, et al. Mammut: A simple architecture for joint learning for multimodal tasks. *arXiv:2303.16839*, 2023. 1, 3

[34] Juho Lee, Yoonho Lee, Jungtaek Kim, Adam R. Kosiorek, Seungjin Choi, and Yee Whye Teh. Set transformer: A framework for attention-based permutation-invariant neural networks. In *ICML*, pages 3744–3753, 2019. 5

[35] Kenton Lee, Mandar Joshi, Iulia Turc, Hexiang Hu, Fangyu Liu, Julian Eisenschlos, Urvashi Khandelwal, Peter Shaw, Ming-Wei Chang, and Kristina Toutanova. Pix2struct: Screenshot parsing as pretraining for visual language understanding. *arXiv:2210.03347*, 2022. 3

[36] Ang Li, Allan Jabri, Armand Joulin, and Laurens Van Der Maaten. Learning visual n-grams from web data. In *ICCV*, pages 4183–4192, 2017. 1, 2

[37] Gang Li and Yang Li. Spotlight: Mobile UI understanding using vision-language models with a focus. In *ICLR*, 2023. 3

[38] Junnan Li, Dongxu Li, Silvio Savarese, and Steven Hoi. BLIP-2: Bootstrapping language-image pre-training with frozen image encoders and large language models. *arXiv:2301.12597*, 2023. 3

[39] Junnan Li, Dongxu Li, Caiming Xiong, and Steven Hoi. BLIP: Bootstrapping language-image pre-training for unified vision-language understanding and generation. In *ICML*, pages 12888–12900, 2022. 1, 3

[40] Junnan Li, Ramprasaath Selvaraju, Akhilesh Gotmare, Shafiq Joty, Caiming Xiong, and Steven Chu Hong Hoi. Align before fuse: Vision and language representation learning with momentum distillation. *NeurIPS*, 34:9694–9705, 2021. 3

[41] Anand Mishra, Shashank Shekhar, Ajeet Kumar Singh, and Anirban Chakraborty. OCR-VQA: Visual Question Answering by Reading Text in Images. In *ICDAR*, 2019. 5

[42] Ron Mokady, Amir Hertz, and Amit H Bermano. Clipcap: Clip prefix for image captioning. *arXiv preprint arXiv:2111.09734*, 2021. 5, 8

[43] Maria-Elena Nilsback and Andrew Zisserman. Automated flower classification over a large number of classes. In *Indian Conf. Computer Vision, Graphics & Image Process.*, pages 722–729, 2008. 5, 17

[44] Hyun Oh Song, Yu Xiang, Stefanie Jegelka, and Silvio Savarese. Deep metric learning via lifted structured feature embedding. In *CVPR*, pages 4004–4012, 2016. 5, 17

[45] Myle Ott, Sergey Edunov, Alexei Baevski, Angela Fan, Sam Gross, Nathan Ng, David Grangier, and Michael Auli. fairseq: A fast, extensible toolkit for sequence modeling. In *Proc. NAACL-HLT: Demonstrations*, 2019. 3

[46] Omkar M. Parkhi, Andrea Vedaldi, Andrew Zisserman, and C. V. Jawahar. Cats and dogs. In *CVPR*, 2012. 5, 17

[47] Hieu Pham, Zihang Dai, Golnaz Ghiasi, Kenji Kawaguchi, Hanxiao Liu, Adams Wei Yu, Jiahui Yu, Yi-Ting Chen, Minh-Thang Luong, Yonghui Wu, Mingxing Tan, and Quoc V. Le. Combined scaling for open-vocabulary image classification. *arXiv:2111.10050*, 2021. 2

[48] Alec Radford, Jong Wook Kim, Chris Hallacy, Aditya Ramesh, Gabriel Goh, Sandhini Agarwal, Girish Sastry, Amanda Askell, Pamela Mishkin, Jack Clark, Gretchen Krueger, and Ilya Sutskever. Learning transferable visual models from natural language supervision. In *ICML*, 2021. 1, 2, 4, 6, 9, 10, 15, 17

[49] Alec Radford, Jeffrey Wu, Rewon Child, David Luan, Dario Amodei, Ilya Sutskever, et al. Language models are unsupervised multitask learners. *OpenAI blog*, 2019. 5, 8

[50] Colin Raffel, Noam Shazeer, Adam Roberts, Katherine Lee, Sharan Narang, Michael Matena, Yanqi Zhou, Wei Li, and Peter J. Liu. Exploring the limits of transfer learning with a unified text-to-text transformer. *J. Mach. Learn. Res.*, 21:140:1–140:67, 2020. 3, 4, 5, 8

[51] Olga Russakovsky, Jia Deng, Hao Su, Jonathan Krause, Sanjeev Satheesh, Sean Ma, Zhiheng Huang, Andrej Karpathy, Aditya Khosla, Michael Bernstein, Alexander C. Berg, and Li Fei-Fei. ImageNet Large Scale Visual Recognition Challenge. *IJCV*, 115(3):211–252, 2015. 5

[52] Mert Bulent Sariyildiz, Julien Perez, and Diane Larlus. Learning visual representations with caption annotations. In *ECCV*, pages 153–170, 2020. 1, 2

[53] Christoph Schuhmann, Richard Vencu, Romain Beaumont, Robert Kaczmarczyk, Clayton Mullis, Aarush Katta, Theo Coombes, Jenia Jitsev, and Aran Komatsuzaki. LAION-400M: Open dataset of CLIP-filtered 400 million image-text pairs. *arXiv:2111.02114*, 2021. 9

[54] Sheng Shen, Liunian Harold Li, Hao Tan, Mohit Bansal, Anna Rohrbach, Kai-Wei Chang, Zhewei Yao, and Kurt Keutzer. How much can CLIP benefit vision-and-language tasks? In *ICLR*, 2022. 3

[55] Mohammad Shoeybi, Mostafa Patwary, Raul Puri, Patrick LeGresley, Jared Casper, and Bryan Catanzaro. Megatron-LM: Training multi-billion parameter language models using model parallelism. *arXiv:1909.08053*, 2019. 3

[56] Quan Sun, Yuxin Fang, Ledell Wu, Xinlong Wang, and Yue Cao. Eva-CLIP: Improved training techniques for CLIP at scale. *arXiv:2303.15389*, 2023. 1

[57] Michael Tschannen, Basil Mustafa, and Neil Houlsby. CLIPPO: Image-and-language understanding from pixels only. In *CVPR*, 2023. 4

[58] Ashish Vaswani, Noam Shazeer, Niki Parmar, Jakob Uszkoreit, Llion Jones, Aidan N. Gomez, Łukasz Kaiser, and Illia Polosukhin. Attention is all you need. In *NeurIPS*, 2017. 2, 3, 8, 15

[59] Catherine Wah, Steve Branson, Peter Welinder, Pietro Perona, and Serge Belongie. The Caltech-UCSD Birds-200-2011 Dataset. 2011. 5, 17

[60] Jianfeng Wang, Zhengyuan Yang, Xiaowei Hu, Linjie Li, Kevin Lin, Zhe Gan, Zicheng Liu, Ce Liu, and Lijuan Wang. GIT: A generative image-to-text transformer for vision and language. *Trans. Machine Learning Research*, 2022. 1, 2, 3, 5

[61] Zirui Wang, Jiahui Yu, Adams Wei Yu, Zihang Dai, Yulia Tsvetkov, and Yuan Cao. SimVLM: Simple visual language model pretraining with weak supervision. In *ICLR*, 2022. 1, 2

[62] Hongwei Xue, Yupan Huang, Bei Liu, Houwen Peng, Jianlong Fu, Houqiang Li, and Jiebo Luo. Probing inter-modality: Visual parsing with self-attention for vision-and-language pre-training. *NeurIPS*, 34:4514–4528, 2021. 3

[63] Peter Young, Alice Lai, Micah Hodosh, and Julia Hockenmaier. From image descriptions to visual denotations: New similarity metrics for semantic inference over event descriptions. *Trans. Assoc. Comput. Linguistics*, 2:67–78, 2014. 5, 6

[64] Jiahui Yu, Zirui Wang, Vijay Vasudevan, Legg Yeung, Mojtaba Seyedhosseini, and Yonghui Wu. Coca: Contrastive captioners are image-text foundation models. *Trans. Machine Learning Research*, 2022. 1, 3, 10

[65] Mert Yuksekogonul, Federico Bianchi, Pratyusha Kalluri, Dan Jurafsky, and James Zou. When and why vision-language models behave like bag-of-words models, and what to do about it? In *ICLR*, 2023. 2, 6, 7, 21

[66] Xiaohua Zhai, Alexander Kolesnikov, Neil Houlsby, and Lucas Beyer. Scaling vision transformers. In *CVPR*, pages 12104–12113, 2022. 4, 5, 8, 15

[67] Xiaohua Zhai, Basil Mustafa, Alexander Kolesnikov, and Lucas Beyer. Sigmoid loss for language image pre-training. *arXiv:2303.15343*, 2023. 2, 4, 5, 6

[68] Xiaohua Zhai, Xiao Wang, Basil Mustafa, Andreas Steiner, Daniel Keysers, Alexander Kolesnikov, and Lucas Beyer. LiT: Zero-shot transfer with locked-image text tuning. In *CVPR*, pages 18102–18112, 2022. 2, 4, 5, 15, 16, 17

[69] Bolei Zhou, Agata Lapedriza, Aditya Khosla, Aude Oliva, and Antonio Torralba. Places: A 10 million image database for scene recognition. *Trans. PAMI*, 2017. 5, 17

A Transfer and finetuning details

Few-shot evaluation We use the linear adaptation protocol and evaluation sets from [66, 68], reporting the 10-shot classification accuracy. Specifically, we rely on the pre-logits layer for CLIP* and GAP of the encoder output sequence for our captioning models. For every combination of data set and model we run the 10-shot adaptation three times and report the mean (and standard deviation for key results).

LiT decoder and T5 decoder To train a multi-task decoder from scratch on top of the frozen representation for classification, captioning and VQA, we precisely follow the setup and hyper parameters from [2] except for the data mixing strategy, for which we set to “concat image-question pairs” ([2, Sec. 5.3]). For all encoders, we use the full feature sequence before pooling (including the class token for the evaluation of CLIP). Throughout, we rely on a B-sized transformer decoder [58] with 12 layers.

For the T5 decoder we keep all the parameters frozen but reinitialize and train the cross-attention layers. We perform a small sweep around the default learning rate and weight decay of the setup used for training from scratch, while keeping the other hyperparameters unchanged.

Linear and non-linear ImageNet-1k probes (frozen transfer) When performing linear and non-linear probes on ImageNet-1k, we run a wide hyper-parameter optimization sweep for all types of probes (linear, MLP, MAP) in order to get solid, trustworthy conclusions. Specifically, for each image encoder and probe combination, we sweep the full cross-product over the following hyper-parameters: **epochs**: (1, 3, 10, 30, 100); **image cropping**: `resize(256) | random_crop(224)` or `inception_crop(224)`; **learning rate**: (0.001, 0.0003, 0.0001) plus earlier runs showing 0.003 and 0.01 to perform much worse; **weight decay**: (0.0001, $lr * 0.1$, 0.0); **hidden dimension**: 0 or 1024; **loss**: sigmoid or softmax cross-entropy. The head weights are always initialized to 0 and its bias to -6.9 in the sigmoid case.

For each result shown in Fig. 3, we select the best setting using 1% of the training data that was held-out for this purpose, and report its accuracy on the 50 000 images in the validation set. For completeness, we further compute various ImageNet test-set variants and report full results in Table 8.

Broad MAP-head transfers (fine-grained) We run the same sweep as described above for each individual dataset and model combination, but only using the MAP-head probe. For each dataset, we either use a provided held-out validation set for selecting the best settings, or hold out 20% of the training set if none is provided. Full numeric results are provided in Table 9. Note that we selected and classified the datasets as coarse- or fine-grained solely by looking at the datasets and their classes, before running any single experiment on them, and never revisited this selection.

Fine-tuning on the full ImageNet-1k data set When fine-tuning on the full ImageNet-1k dataset, we attach a fresh MAP head to the pretrained encoder and run full fine-tuning using the AdaFactor optimizer modified for ViTs in [66]. In each setting (B/16, B/16₃₈₄, L/14₃₃₆), we run the exact same sweep for CLIP*, CapPa, and Cap models. Notably, our exploration is significantly smaller than that of [14] and unlike for CLIP [48], ImageNet was fully de-duplicated from our pre-training dataset. In all cases, we select the best model on a held-out 2% of the training data and report that model’s performance on the 50 000 image validation set without re-training.

For the B/16 models, we sweep over three **learning rates**: (0.0001, 0.0003, 0.00001); two **layer-wise learning-rate decays**: (None, 0.8); 2 **RandAugment** parameters: (10, 15); 3 **Mixup**: (0.0, 0.2, 0.5); and five **Polyak (EMA) averaging factors**: (None, 0.9, 0.999, 0.99999, 0.999999) with a batch size of 2048 and 100 epochs. The best setting uses learning rate 0.00001, layer-wise decay 0.8, Mixup 0.5 and no Polyak averaging.

For the L/14 models at 336 px resolution, we sweep over three **learning rates**: (0.001, 0.0003, 0.0001), three **layer-wise learning-rate decays**: (None, 0.9, 0.8), and five **Polyak (EMA) averaging factors**: (None, 0.9, 0.999, 0.99999, 0.999999). Note that the latter does not require re-training for each setting and hence is cheap. We fix rand-augment to (2, 10), Mixup to 0.2, and training duration to 50 000 steps with batch-size 512, without revisiting these choices. Besides that, we mostly follow [15, 66]. The best setting uses learning rate 0.0001, layer-wise decay 0.9, and Polyak 0.99999 for both models.

B Additional Results

B.1 Probing and LiT tuning results

Table 8 shows the classification accuracy on different ImageNet-1k evaluation sets, when probing the frozen representation with different probes (linear and non-linear), extending the numerical results from Fig. 3.

Table 9 presents transfer results of the frozen representation to fine- and coarse-grained classification tasks (using a MAP head). This complements the results from Fig. 4 (Right).

Table 10 expands Table 4 in the main paper and shows frozen transfer for zero-shot classification and retrieval via LiT [68].

Table 11 presents the performance of frozen Cap/Cap and CLIP* encoders when combined via cross-attention with a *frozen* T5 decoder. This represents the data from Fig. 4 (Left) in the main paper in tabular form.

Table 8: Extended numerical results for Fig. 3, i.e. linear and non-linear ImageNet-1k probes on top of the frozen models. While the *linear* separability of CLIP models is higher, the gap between CLIP* and Cap models is mostly closed when the probe also learns how to pool (*map*).

| Model | Head | Top-1 | ReaL | -v2 | -R(edition) | -A(dvers.) | ObjectNet |
|-------------|---------|-------|------|------|-------------|------------|-----------|
| CLIP* (8k) | linear | 79.8 | 85.6 | 69.0 | 71.9 | 38.0 | 49.8 |
| | mlp | 80.4 | 86.1 | 69.6 | 74.4 | 39.3 | 50.9 |
| | map | 82.2 | 87.3 | 71.5 | 72.9 | 34.3 | 49.0 |
| | map+mlp | 82.2 | 87.4 | 71.7 | 71.8 | 34.8 | 48.3 |
| CLIP* (16k) | linear | 80.2 | 85.9 | 69.2 | 73.2 | 40.3 | 51.3 |
| | mlp | 80.9 | 86.1 | 70.3 | 71.4 | 37.3 | 49.8 |
| | map | 82.6 | 87.5 | 72.4 | 73.9 | 37.2 | 50.0 |
| | map+mlp | 82.6 | 87.5 | 72.1 | 73.0 | 36.3 | 49.3 |
| Cap | linear | 77.7 | 84.1 | 67.1 | 68.2 | 24.1 | 44.2 |
| | mlp | 78.5 | 84.8 | 68.0 | 76.0 | 27.1 | 45.6 |
| | map | 81.6 | 87.0 | 71.3 | 76.2 | 32.3 | 45.8 |
| | map+mlp | 81.5 | 87.0 | 71.5 | 76.2 | 31.4 | 45.8 |
| CapPa | linear | 78.3 | 84.6 | 66.5 | 67.7 | 22.1 | 43.7 |
| | mlp | 79.4 | 85.6 | 68.6 | 77.2 | 25.6 | 46.2 |
| | map | 82.0 | 87.5 | 72.3 | 80.9 | 41.5 | 50.1 |
| | map+mlp | 82.1 | 87.3 | 72.0 | 79.4 | 39.1 | 49.5 |
| CLIP* L/14 | linear | 84.2 | 88.4 | 75.0 | 83.8 | 59.1 | 60.2 |
| | mlp | 84.6 | 88.5 | 74.9 | 83.3 | 56.6 | 58.6 |
| | map | 85.9 | 89.3 | 76.7 | 84.9 | 57.4 | 58.2 |
| | map+mlp | 85.8 | 89.2 | 77.0 | 83.6 | 56.1 | 57.8 |
| CapPa L/14 | linear | 83.0 | 87.7 | 73.1 | 81.1 | 41.6 | 53.8 |
| | mlp | 84.1 | 88.7 | 74.6 | 87.3 | 47.0 | 56.8 |
| | map | 85.8 | 89.3 | 76.8 | 86.1 | 54.5 | 56.6 |
| | map+mlp | 85.8 | 89.2 | 76.6 | 85.5 | 52.2 | 56.5 |

Table 9: Transfer of the frozen representation to fine- and coarse-grained classification tasks (using a MAP head). This extends the numerical results of Figure 4 (Right).

| Dataset | Grain | CLIP* (8k) | CLIP* (16k) | Cap | CapPa | CLIP* L/14 | CapPa L/14 |
|---------------|--------|------------|-------------|------|-------|------------|------------|
| Dogs [27] | Fine | 77.5 | 77.9 | 79.6 | 81.2 | 85.0 | 86.0 |
| Flowers [43] | Fine | 85.1 | 89.5 | 94.0 | 97.0 | 96.6 | 98.9 |
| Birds [59] | Fine | 76.9 | 78.1 | 76.3 | 54.2 | 85.0 | 86.7 |
| Pets [46] | Fine | 91.2 | 91.2 | 91.5 | 94.4 | 94.4 | 95.4 |
| Cars [31] | Fine | 90.8 | 91.6 | 93.4 | 93.3 | 94.0 | 95.8 |
| Food [3] | Fine | 91.0 | 92.1 | 91.1 | 91.5 | 94.9 | 94.2 |
| RESISC [8] | Coarse | 92.5 | 96.4 | 90.5 | 96.1 | 97.1 | 96.9 |
| Products [44] | Coarse | 88.8 | 89.0 | 87.8 | 88.5 | 90.7 | 90.3 |
| SUN397 [69] | Coarse | 81.8 | 82.9 | 82.0 | 82.1 | 85.7 | 85.2 |
| Caltech [19] | Coarse | 93.5 | 93.1 | 89.0 | 86.5 | 93.8 | 93.2 |
| STL-10 [12] | Coarse | 98.0 | 98.5 | 97.7 | 98.1 | 99.2 | 99.1 |
| Cat/Dog [18] | Coarse | 99.9 | 99.9 | 99.7 | 99.7 | 99.8 | 99.9 |

Table 10: Frozen transfer for zero-shot classification and retrieval via LiT [68] as a function of the number of training examples seen by the text encoder (the vision encoder is pretrained and frozen, and equipped with a MAP head which is trained along with the text encoder). The text encoder mirrors the architecture of the vision encoder. Especially for the larger model, CapPa is competitive with CLIP* with comparable or fewer examples seen. The CLIP numbers are obtained by evaluating the image and text encoders released by [48] in our eval setup. We report these numbers for reference, no LiT tuning is done on top of the CLIP vision encoder. This table complements Table 4 in the main paper.

| LiT pairs: | ImageNet 0shot | | | | COCO t2i r@1 | | | | COCO i2t r@1 | | | |
|-------------|----------------|------|------|------|--------------|------|------|------|--------------|------|------|------|
| | 0 | 900M | 3B | 12B | 0 | 900M | 3B | 12B | 0 | 900M | 3B | 12B |
| Cap | - | 65.9 | 67.8 | 69.0 | - | 35.3 | 37.5 | 39.1 | - | 50.3 | 53.9 | 54.8 |
| CapPa | - | 66.4 | 68.8 | 70.2 | - | 34.3 | 37.3 | 38.6 | - | 49.7 | 53.9 | 55.1 |
| CLIP* (8k) | 65.6 | 65.9 | 67.6 | 69.0 | 41.5 | 36.5 | 38.2 | 39.5 | 56.7 | 52.0 | 54.0 | 56.1 |
| CLIP* (16k) | 67.7 | 66.7 | 69.0 | 70.0 | 43.0 | 37.0 | 38.9 | 40.1 | 58.2 | 53.0 | 55.1 | 57.0 |
| CLIP | | | 68.3 | | | | 32.3 | | | | 52.8 | |
| CapPa L/14 | - | 74.6 | 76.4 | 77.5 | - | 40.6 | 43.9 | 45.4 | - | 56.6 | 60.3 | 62.6 |
| CLIP* L/14 | 74.8 | 74.5 | 75.8 | 76.6 | 48.1 | 42.7 | 44.7 | 46.3 | 63.7 | 57.7 | 60.7 | 62.3 |
| CLIP L/14 | | | 75.1 | | | | 36.5 | | | | 56.6 | |

Table 11: Performance of frozen representations trained via image captioning (Cap/CapPa) and contrastive (CLIP*) objective, when combined via cross-attention with a *frozen* T5 decoder. Only the cross-attention weights are updated during the training. See Table 2 for the corresponding models that have the decoder trained from scratch.

| | Classification | | | | | Captioning | | OCR | | Question Ans. | |
|-------------|----------------|----------------|----------------|----------------|----------------|-----------------|----------------|----------------|----------------|----------------|--|
| | i1k | sun | food | res | pet | COCO | Flickr | VQA | VQAv2 | GQA | |
| Cap | 79.0 \pm 0.1 | 81.3 \pm 0.1 | 89.3 \pm 0.0 | 92.4 \pm 0.1 | 92.3 \pm 0.3 | 119.7 \pm 0.6 | 72.2 \pm 0.9 | 57.7 \pm 0.0 | 64.6 \pm 0.1 | 52.1 \pm 0.2 | |
| CapPa | 80.0 \pm 0.0 | 81.2 \pm 0.1 | 89.9 \pm 0.0 | 93.1 \pm 0.2 | 93.2 \pm 0.3 | 118.7 \pm 0.5 | 70.0 \pm 0.5 | 57.8 \pm 0.2 | 63.3 \pm 0.3 | 51.9 \pm 0.3 | |
| CLIP* (8k) | 79.1 \pm 0.0 | 81.5 \pm 0.2 | 89.9 \pm 0.0 | 92.7 \pm 0.2 | 88.5 \pm 0.2 | 110.6 \pm 0.5 | 60.8 \pm 1.0 | 50.3 \pm 0.3 | 57.2 \pm 0.4 | 49.5 \pm 0.2 | |
| CLIP* (16k) | 79.5 \pm 0.1 | 81.7 \pm 0.1 | 90.4 \pm 0.1 | 93.7 \pm 0.0 | 88.6 \pm 0.1 | 110.6 \pm 0.6 | 59.8 \pm 0.9 | 50.2 \pm 0.4 | 56.8 \pm 0.3 | 49.6 \pm 0.3 | |

B.2 Scaling properties

Fig. 8 and 9 show the performance of frozen Cap, CapPa, and CLIP* encoders on a variety of tasks as a function of the number of training examples seen and the encoder model size, respectively. Specifically, we evaluate our models on classification, captioning, and VQA when combined with a decoder trained from scratch to solve all those tasks jointly (following [2]), and on 10-shot linear classification based on the pre-logit features.

Tables 12, 13 and 14, 15 show the data from Fig. 8 and 9, respectively, in tabular form. For completeness, in Table 15 we also present the ImageNet zero-shot accuracy (without prompts) of CapPa and CLIP* models obtained with their respective pretrained decoder and encoder. We emphasize that scoring-based zero-shot classification is not the focus of this paper, and we did not optimize the Cap/CapPa models for this.

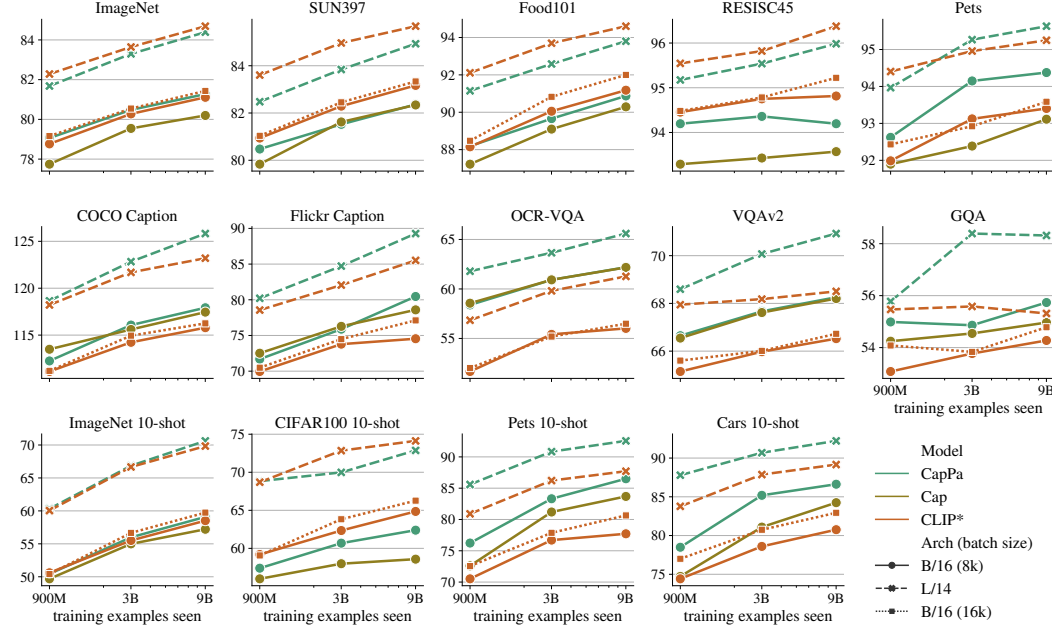


Figure 8: Performance of vision backbones pre-trained with captioning (Cap/CapPa) and contrastive objective (CLIP*) as a function of the number of pre-training examples seen (expands the results in Fig. 2). **Top two rows:** Classification, captioning, and VQA performance with a decoder trained from scratch in multi-task fashion (see [2] for details). We use CIDEr for captioning, the VQAv2 weighted accuracy for VQAv2, and exact matching accuracy for all other tasks. **Bottom row:** 10-shot linear classification accuracy on the frozen pre-logit representation.

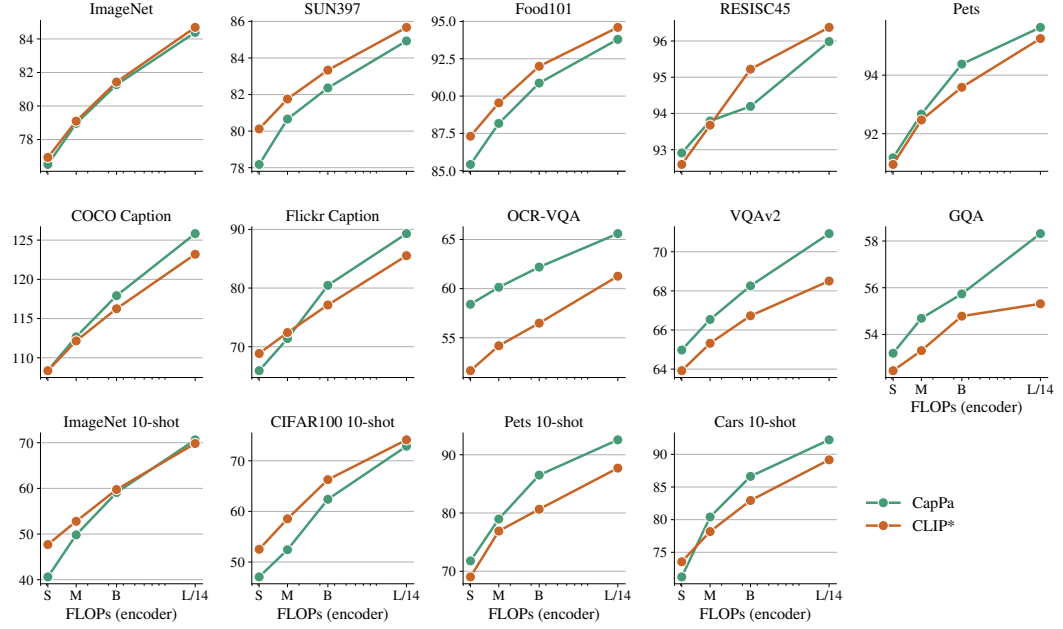


Figure 9: Performance of vision backbones pre-trained with captioning (CapPa) and contrastive objective (CLIP*) as a function of the model size/FLOPs (we compare ViT-S/16, M/16, B/16, and L/14; this expands the results in Fig. 2). **Top two rows:** Classification, captioning, and VQA performance with a decoder trained from scratch in multi-task fashion (see [2] for details). We use CIDEr for captioning, the VQAv2 weighted accuracy for VQAv2, and exact matching accuracy for all other tasks. **Bottom row:** 10-shot linear classification accuracy on the frozen pre-logit representation.

Table 12: Data corresponding to Fig. 8 (top two rows) in tabular form. See caption of Fig. 8 for details on the metrics.

| ex. | seen | model | arch | Classification | | | | | Captioning | | OCR | Question Ans. | |
|------|-------|-------|-------|----------------|------|------|------|------|------------|--------|------|---------------|------|
| | | | | i1k | sun | food | res | pet | COCO | Flickr | VQA | VQAv2 | GQA |
| 900M | Cap | B/16 | (8k) | 77.7 | 79.8 | 87.2 | 93.3 | 91.9 | 113.5 | 72.5 | 58.6 | 66.5 | 54.2 |
| | | B/16 | (8k) | 79.1 | 80.5 | 88.2 | 94.2 | 92.6 | 112.2 | 71.7 | 58.4 | 66.6 | 55.0 |
| | | L/14 | | 81.7 | 82.5 | 91.1 | 95.2 | 94.0 | 118.7 | 80.2 | 61.8 | 68.6 | 55.8 |
| | CLIP* | B/16 | (8k) | 78.8 | 80.9 | 88.2 | 94.5 | 92.0 | 111.1 | 70.0 | 51.7 | 65.1 | 53.1 |
| | | B/16 | (16k) | 79.2 | 81.0 | 88.5 | 94.5 | 92.4 | 111.2 | 70.5 | 52.0 | 65.6 | 54.1 |
| 3B | Cap | B/16 | (8k) | 79.5 | 81.6 | 89.1 | 93.4 | 92.4 | 115.6 | 76.3 | 60.9 | 67.6 | 54.5 |
| | | B/16 | (8k) | 80.5 | 81.5 | 89.7 | 94.4 | 94.1 | 116.1 | 75.9 | 60.9 | 67.7 | 54.9 |
| | | L/14 | | 83.3 | 83.8 | 92.6 | 95.5 | 95.3 | 122.8 | 84.7 | 63.7 | 70.1 | 58.4 |
| | CLIP* | B/16 | (8k) | 80.3 | 82.3 | 90.1 | 94.8 | 93.1 | 114.2 | 73.8 | 55.4 | 66.0 | 53.8 |
| | | B/16 | (16k) | 80.5 | 82.5 | 90.8 | 94.8 | 92.9 | 114.9 | 74.5 | 55.2 | 66.0 | 53.8 |
| 9B | Cap | B/16 | (8k) | 80.2 | 82.3 | 90.3 | 93.6 | 93.1 | 117.5 | 78.6 | 62.2 | 68.2 | 55.0 |
| | | B/16 | (8k) | 81.3 | 82.4 | 90.9 | 94.2 | 94.4 | 117.9 | 80.5 | 62.2 | 68.3 | 55.7 |
| | | L/14 | | 84.4 | 84.9 | 93.8 | 96.0 | 95.6 | 125.8 | 89.3 | 65.6 | 70.9 | 58.3 |
| | CLIP* | B/16 | (8k) | 81.1 | 83.2 | 91.2 | 94.8 | 93.4 | 115.8 | 74.5 | 56.0 | 66.5 | 54.3 |
| | | B/16 | (16k) | 81.4 | 83.3 | 92.0 | 95.2 | 93.6 | 116.3 | 77.1 | 56.5 | 66.7 | 54.8 |
| | | L/14 | | 84.7 | 85.7 | 94.6 | 96.4 | 95.2 | 123.2 | 85.5 | 61.3 | 68.5 | 55.3 |

Table 13: Data corresponding to Fig. 8 (bottom row) in tabular form. 10-shot linear classification accuracy on the frozen pre-logit features.

| ex. seen | model | arch | ImageNet | CIFAR100 | Pets | Cars |
|----------|-------|------------|----------|----------|------|------|
| 900M | Cap | B/16 (8k) | 49.7 | 56.0 | 72.6 | 74.7 |
| | CapPa | B/16 (8k) | 50.4 | 57.4 | 76.2 | 78.5 |
| | | L/14 | 60.3 | 68.8 | 85.6 | 87.8 |
| | | B/16 (8k) | 50.6 | 59.2 | 70.5 | 74.4 |
| | CLIP* | B/16 (16k) | 50.4 | 59.1 | 72.6 | 77.0 |
| | | L/14 | 60.0 | 68.7 | 80.9 | 83.8 |
| 3B | Cap | B/16 (8k) | 55.0 | 58.0 | 81.2 | 81.1 |
| | CapPa | B/16 (8k) | 56.0 | 60.7 | 83.3 | 85.2 |
| | | L/14 | 66.9 | 70.0 | 90.8 | 90.7 |
| | | B/16 (8k) | 55.5 | 62.3 | 76.7 | 78.6 |
| | CLIP* | B/16 (16k) | 56.7 | 63.8 | 77.9 | 80.7 |
| | | L/14 | 66.7 | 72.8 | 86.2 | 87.9 |
| 9B | Cap | B/16 (8k) | 57.2 | 58.6 | 83.7 | 84.2 |
| | CapPa | B/16 (8k) | 59.1 | 62.4 | 86.5 | 86.6 |
| | | L/14 | 70.6 | 72.9 | 92.6 | 92.2 |
| | | B/16 (8k) | 58.5 | 64.9 | 77.7 | 80.8 |
| | CLIP* | B/16 (16k) | 59.7 | 66.3 | 80.6 | 82.9 |
| | | L/14 | 69.8 | 74.1 | 87.7 | 89.2 |

Table 14: Data corresponding to Fig. 9 (top two rows) in tabular form. See caption of Fig. 9 for details on the metrics

| arch | FLOPs | model | Classification | | | | Captioning | | OCR | Question Ans. | | |
|------|--------|-------|----------------|------|------|------|------------|-------|--------|---------------|-------|------|
| | | | i1k | sun | food | res | pet | COCO | Flickr | VQA | VQAv2 | GQA |
| S/16 | 9.2G | CapPa | 76.5 | 78.2 | 85.4 | 92.9 | 91.2 | 108.4 | 65.9 | 58.4 | 65.0 | 53.2 |
| | | CLIP* | 76.9 | 80.1 | 87.3 | 92.6 | 91.0 | 108.4 | 68.8 | 51.7 | 63.9 | 52.4 |
| M/16 | 16.0G | CapPa | 79.0 | 80.7 | 88.2 | 93.8 | 92.7 | 112.7 | 71.4 | 60.1 | 66.5 | 54.7 |
| | | CLIP* | 79.1 | 81.8 | 89.5 | 93.7 | 92.5 | 112.2 | 72.4 | 54.2 | 65.3 | 53.3 |
| B/16 | 35.1G | CapPa | 81.3 | 82.4 | 90.9 | 94.2 | 94.4 | 117.9 | 80.5 | 62.2 | 68.3 | 55.7 |
| | | CLIP* | 81.4 | 83.3 | 92.0 | 95.2 | 93.6 | 116.3 | 77.1 | 56.5 | 66.7 | 54.8 |
| L/14 | 161.8G | CapPa | 84.4 | 84.9 | 93.8 | 96.0 | 95.6 | 125.8 | 89.3 | 65.6 | 70.9 | 58.3 |
| | | CLIP* | 84.7 | 85.7 | 94.6 | 96.4 | 95.2 | 123.2 | 85.5 | 61.3 | 68.5 | 55.3 |

Table 15: Data corresponding to Fig. 9 (bottom row) in tabular form. 10-shot linear classification accuracy on the frozen pre-logit features. We also show the ImageNet zero-shot classification accuracy (without prompts) when using the pretrained text encoder (CLIP*) or text decoder with scoring (CapPa) for reference (last column).

| arch | FLOPs | model | ImageNet | CIFAR100 | Pets | Cars | ImageNet zs. |
|------|--------|-------|----------|----------|------|------|--------------|
| S/16 | 9.2G | CapPa | 40.6 | 47.1 | 71.8 | 71.2 | 35.1 |
| | | CLIP* | 47.7 | 52.5 | 69.0 | 73.6 | 52.8 |
| M/16 | 16.0G | CapPa | 49.8 | 52.4 | 79.0 | 80.4 | 43.0 |
| | | CLIP* | 52.8 | 58.5 | 76.9 | 78.2 | 58.7 |
| B/16 | 35.1G | CapPa | 59.1 | 62.4 | 86.5 | 86.6 | 52.7 |
| | | CLIP* | 59.7 | 66.3 | 80.6 | 82.9 | 64.1 |
| L/14 | 161.8G | CapPa | 70.6 | 72.9 | 92.6 | 92.2 | 63.8 |
| | | CLIP* | 69.8 | 74.1 | 87.7 | 89.2 | 71.2 |

B.3 Attribution, relation, ordering

Table 16 shows extended results for different models on the ARO benchmark [65] (see Table 6 in the main paper). In addition to the clear superiority of Cap/CapPa over CLIP* models discussed in the main paper, it can be observed that increasing the model capacity from B/16 to L/14 leads to an overall improvement for CapPa, while this is not the case for CLIP*.

Table 16: Results on the Attribute, Relation and Order (ARO) benchmark [65]. Cap and CapPa models clearly outperform all CLIP* and CLIP variants across all data sets, even when training the model to be sensitive to word ordering and attribution as in NegCLIP [65]. Values for “ARO Best” are taken from [65]. “Blind dec.” corresponds to Cap without vision encoder, i.e. the vision encoder features fed to the decoder are replaced with all zeros.

| | Arch | VG Attribution | VG Relation | Flickr Order | COCO Order |
|-------------|------|----------------|-------------|--------------|------------|
| Blind dec. | - | 83.7 | 86.2 | 98.8 | 98.7 |
| Cap | B/16 | 88.9 | 86.6 | 99.1 | 99.0 |
| CapPa | B/16 | 85.7 | 86.7 | 99.2 | 98.8 |
| CapPa | L/14 | 89.3 | 86.0 | 99.3 | 99.0 |
| CLIP* (8k) | B/16 | 55.4 | 39.8 | 43.7 | 32.8 |
| CLIP* (16k) | B/16 | 53.2 | 39.7 | 45.5 | 37.0 |
| CLIP* (16k) | L/14 | 57.8 | 35.9 | 40.2 | 31.5 |
| CLIP | B/32 | 63.2 | 59.1 | 59.4 | 47.3 |
| CLIP | B/16 | 62.7 | 58.7 | 57.9 | 49.5 |
| ARO Best | - | 88.0 | 73.0 | 60.0 | 46.0 |
| NegCLIP | B/32 | 71.0 | 81.0 | 91.0 | 86.0 |

B.4 Ablations

Table 17 compares the performance of the CapPa and CLIP* vision encoders with a ViT-B/16 pretrained in supervised fashion on ImageNet-21k when combined with transformer decoder. Table 18 represents the data from Fig. 7 in tabular form.

Table 17: Comparison of CapPa and CLIP* with a ViT-B/16 pretrained in supervised fashion on ImageNet-21k (we use the checkpoint from Steiner et al. 2021) when combined with a transformer decoder trained from scratch for classification, captioning, and VQA [2]. CLIP* and CapPa outperform the model pretrained in supervised fashion.

| | Classification | | | | | Captioning | | OCR | | Question Ans. | |
|-----------------|----------------|----------------|----------------|----------------|----------------|-----------------|----------------|----------------|----------------|----------------|--|
| | i1k | sun | food | res | pet | COCO | Flickr | VQA | VQAv2 | GQA | |
| ViT-B/16 (i21k) | 73.1 ± 0.1 | 72.8 ± 0.2 | 81.2 ± 0.2 | 86.2 ± 0.1 | 85.6 ± 0.3 | 95.0 ± 0.4 | 52.3 ± 0.1 | 39.1 ± 0.1 | 57.6 ± 0.3 | 50.1 ± 0.1 | |
| CapPa | 81.3 ± 0.1 | 82.4 ± 0.1 | 90.9 ± 0.1 | 94.2 ± 0.2 | 94.4 ± 0.1 | 117.9 ± 0.6 | 80.5 ± 0.2 | 62.2 ± 0.0 | 68.3 ± 0.1 | 55.7 ± 0.2 | |
| CLIP* | 81.4 ± 0.1 | 83.3 ± 0.1 | 92.0 ± 0.1 | 95.2 ± 0.2 | 93.6 ± 0.2 | 116.3 ± 0.7 | 77.1 ± 0.7 | 56.5 ± 0.1 | 66.7 ± 0.1 | 54.8 ± 0.6 | |

Table 18: Ablation results representing Fig. 7 in tabular form. **Left:** 10-shot linear classification accuracy based on the frozen encoder representation as a function of the fraction of training batches for which parallel prediction is performed in CapPa. **Right:** 10-shot linear classification accuracy and zero-shot classification accuracy as a function of the vision encoder architecture.

| fraction | INet | C100 | Pets | Cars | arch | model | INet | C100 | Pets | Cars | INet zs. |
|----------|------|------|------|------|----------|------------|------|------|------|------|----------|
| 0% | 49.7 | 56.0 | 72.6 | 74.7 | R50 | CLIP* (8k) | 39.8 | 33.5 | 49.2 | 60.9 | 43.6 |
| 25% | 46.7 | 52.9 | 71.9 | 72.8 | | Cap | 37.8 | 33.3 | 48.6 | 52.4 | 28.5 |
| 50% | 49.8 | 57.8 | 76.8 | 76.9 | ViT-B/32 | CLIP* (8k) | 44.1 | 57.7 | 64.7 | 68.1 | 48.3 |
| 75% | 50.4 | 57.4 | 76.2 | 78.5 | | Cap | 41.0 | 53.7 | 64.0 | 58.7 | 35.4 |
| 90% | 49.0 | 59.5 | 73.1 | 79.0 | ViT-B/16 | CLIP* (8k) | 50.6 | 59.2 | 70.5 | 74.4 | 52.2 |
| | | | | | | Cap | 49.7 | 56.0 | 72.6 | 74.7 | 43.8 |